Biosensors and Bioelectronics 156 (2020) 112128

Contents lists available at ScienceDirect

Biosensors and Bioelectronics

journal homepage: http://www.elsevier.com/locate/bios

Donor effect dominated molybdenum disulfide/graphene nanostructure-based field-effect transistor for ultrasensitive DNA detection

Shuo Chen [a,1], Yang Sun [a,b,1], Yaping Xia [a], Ke Lv [a], Baoyuan Man [a,**], Cheng Yang [a,b,*]

[a] School of Physics and Electronics, Shandong Normal University, Jinan, 250014, People's Republic of China
[b] Department of Electrical Engineering, University at Buffalo North Campus, Buffalo, NY, 14260, USA

ARTICLE INFO

Keywords:
DNA sensing
MoS_2/Graphene nanostructure
Field effect transistor
Donor effect

ABSTRACT

Field effect transistor (FET) biosensors based on low-dimensional materials have the advantages of small in size, simple structure, fast response and high sensitivity. In this work, a field-effect transistor biosensor based on molybdenum disulfide/graphene (MoS_2/graphene) hybrid nanostructure was proposed and fabricated for DNA hybridization detection. The biosensor achieved an effective response to DNA concentrations in a broad range from 10 aM to 100 pM and a limit of detection (LOD) of 10 aM was obtained, which was one or more orders of magnitude lower than the reported result. The sensing mechanisms (donor and gating effects) of the FET sensor were discussed. A larger voltage shift of the charge neutral point was obtained due to a strengthened donor effect and a weakened gating effect caused by the introduction of MoS_2 layers. Such FET sensor shows high specificity for different matching degrees of complementary DNA, indicating the potential use of such a sensor in disease diagnosis.

1. Introduction

DNA plays a vital role in biology as the carrier of genetic information in all living species. It has been proposed that DNA detection can predict disease risk and achieve targeted prevention (Long et al., 2014). In order to effectively combat diseases, accurate detection of DNA sequences is particularly important (Kelley et al., 2014). Therefore, it is urgent to develop a sensitive DNA detection method. In the past few decades, many new DNA detection methods with high sensitivity and specificity have emerged based on the FET sensor with the advantages of ultra-sensitivity, fast response and automatic high flux detection (Cai et al., 2014; Kaisti, 2017; Xu et al., 2017).

Usually, the sensing materials of the FET sensors are made of low-dimensional materials (such as one-dimensional silicon nanowires or carbon nanotubes (Fradetal et al., 2016; Jayakumar et al., 2019; Khosravi et al., 2017; Sun et al., 2019), and two dimensional graphene (Du et al., 2008; Gao et al., 2018). Graphene-based FET sensors, where DNA with a negatively charged group can modulate the density of the graphene carrier, causing doping of the graphene layers, became the focus of research (Kim et al., 2013; Yue et al., 2017). In these, a voltage shift of the charge neutral point caused by changes in the Fermi level is viewed as the detection signal (Campos et al., 2019; Xu et al., 2017). However, practical biomolecular detection is performed in an aqueous solution, and water molecules easily affect the Fermi level of graphene, which works as an external perturbation and brings signal noise (Loan et al., 2014; Schedin et al., 2007). In a water environment, the Debye shielding effect causes the carrier density of the sensing material to be modulated only partly by the DNA negative group (Nakatsuka et al., 2018; Stern et al., 2007), which causes DNA to not be fully detected and causes weak detection signal. MoS_2 can easily induce polarization of DNA molecules, reduce the distance between DNA and the sensing materials (Wu et al., 2013), and can easily be coated onto the graphene surface by van der Waals interactions to be used as a protective layer (Yang et al., 2015; Zhou et al., 2014). Therefore, a MoS_2/graphene hybrid nanostructure was fabricated here to weaken the non-ideal effects caused by the Debye shielding effect and avoid the noise caused by water.

We were the first to propose MoS_2/graphene hybrid nanostructures for the ultra-sensitive detection of DNA hybridization. The sensing mechanism, benefiting from the introduction of MoS_2 layers, was analyzed by experimental and theoretical methods. Limit of detection

* Corresponding author. School of Physics and Electronics, Shandong Normal University, Jinan, 250014, People's Republic of China.
** Corresponding author.
E-mail addresses: byman@sdnu.edu.cn (B. Man), chengyang@sdnu.edu.cn (C. Yang).
[1] These authors are contributed equally.

https://doi.org/10.1016/j.bios.2020.112128
Received 15 December 2019; Received in revised form 25 February 2020; Accepted 27 February 2020
Available online 3 March 2020

(LOD) of 10 aM was obtained, which provides an excellent avenue for detecting the target DNA molecules. In addition, the MoS_2/graphene nanostructure FET biosensor can accurately identify complementary DNA with five matching degrees. As a result, this new type of sensing device may be used as a testing tool for disease diagnosis.

2. Experimental section

2.1. Materials

Phosphate buffer solution (PBS), ethanolamine and 1-pyrenebutanoic acid succinimidyl ester (PBASE) were purchased from Aladdin. All other regents were ordered from Sinopharm Chemical Reagent Co., Ltd. Ultrapure water was obtained from a Millipore water purification system (Milli-Q Direct8). DNA samples were purchased from Sangon Biotech (Shanghai) Co. Ltd.

2.2. MoS_2/graphene nanostructure FET fabrication

The fabrication process of the MoS_2/graphene nanostructure FET has been shown in Fig. 1. Firstly, graphene, used as a sensing substrate, was prepared by chemical vapor deposition (CVD) in our lab. Secondly, polymethylmethacrylate (PMMA), a support layer to prevent graphene tearing, was coated on a graphene/copper substrate. A redox reaction was used to remove the copper. Acetone, ethanol and DI water were used to ensure the complete removal of PMMA. Then, graphene was transferred to a SiO_2/Si substrate, where indium tin oxide (ITO) electrodes were used as the source/drain electrodes of graphene FET and the area of the sensing channel was 1 cm × 0.4 mm. Next, an $(NH_4)_2MoS_4$ (purity of 99.99%) solution of 0.06 g/ml was spin-coated onto the graphene surface at 4000 r/s for an optimized time of 30 s. Finally, annealing process with 500 °C for 30 min was used to form MoS_2. The reaction principle is as follows:

$$(NH_4)_2MoS_4 + H_2 \rightarrow 2NH_3 + 2H_2S + MoS_2 \text{ (at 500 °C, 30 min)}$$

2.3. Device functionalization and DNA hybridization

To immobilize the Probe DNA on the hybrid nanostructure surfaces and avoid the loss of carrier mobility, PBASE dissolved in N,N-dimethylformamide (DMF) was used as the connector of the Probe DNA and the hybrid nanostructure. The PBASE linker binds to MoS_2 by π stacking (non-covalent interaction) of its pyrene group onto the MoS_2 surface, while the succinimide portion of PBASE protrudes from the sensor surface and immobilized 5′-amine-modified Probe DNA through the conjugated reaction between the amine group of Probe DNA and the amine-reactive succinimide group of PBASE. 10 mM PBASE solution was added to the FET devices to effectively fix Probe DNA on the MoS_2 surface. Then, DMF solution was used to remove the extra PBASE. Next, 5′-amino-modified probe DNA with a concentration of 1 μM was dropped onto the sensing material surface to react with the PBASE, and non-bound DNA was rinsed off with 1 × PBS buffer solution. Finally, 100 mM ethanolamine was used to inactivate the excess reactive groups of PBASE for 1 h, which prevents possible nonspecific binding events, and was then rinsed with DI water. After the above steps, the MoS_2/graphene hybrid nanostructure FET sensor was completely functionalized. DNA hybridization was conducted by dropping an appropriate concentration of a fully complementary DNA (FC DNA) solution onto the device and incubating for 6 h. Probe DNA were immobilized on the MoS_2 surface through non-covalent bonds. To confirm specificity, the same procedure was repeated using different matching degrees of complementary DNA instead of FC DNA to perform the hybridization with the Probe DNA.

2.4. Characterization

The electrical properties of the MoS_2/graphene FET were determined using a Keithley 4200-SCS semiconductor parameter analyzer. To measure the I_{ds}-V_g (I_{ds} is the drain-source current, V_g is the gate voltage) curve of the hybrid nano structure devices, an Ag/AgCl wire was used as the gate electrode and a constant bias V_{ds} = 0.1 V (the drain-source voltage) was applied. Scanning electron microscopy (SEM, Zeiss Gemini Ultra-55) was used to characterize the morphologies of the samples at a 5 KV acceleration voltage for accurately distinguishing the subtle changes in the characteristic peaks of MoS_2/graphene. The Raman instrument used in this study was a Horiba HR Evolution 800

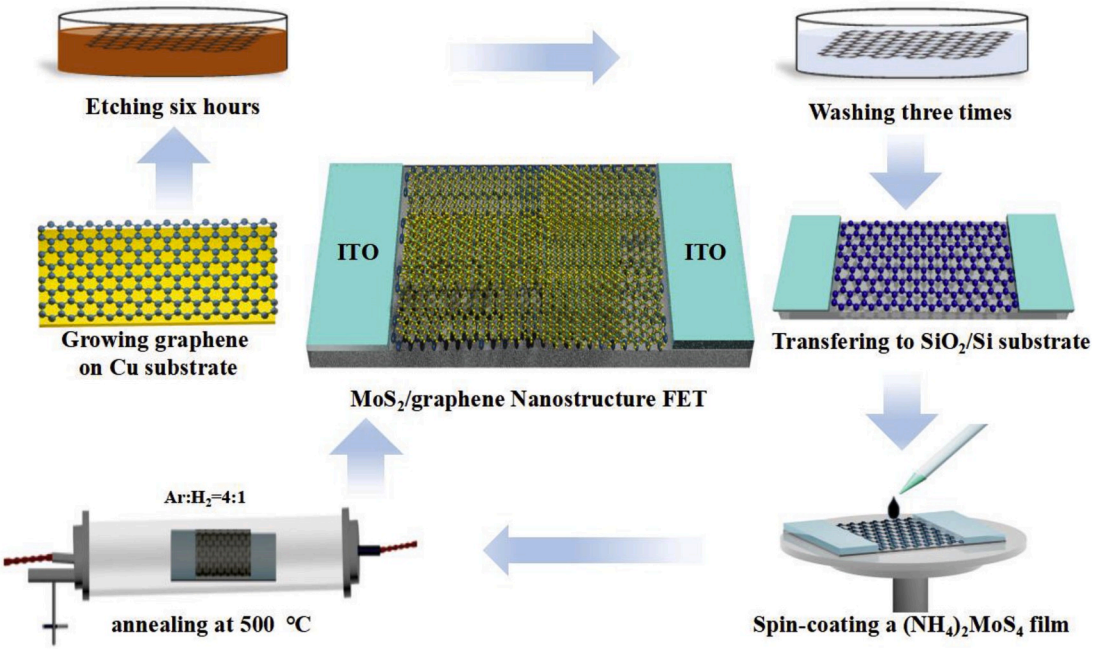

Fig. 1. Schematic of MoS_2/graphene nanostructure FET fabrication.

with excitation by a laser (532 nm). The laser power was set to 0.5 mW to avoid sample heating and photo-induced damage. The laser beam was focused on the sample with an area of 1 μm^2.

3. Results and discussion

3.1. Working principle and characterization of MoS_2/graphene nanostructure

DNA hybridization was detected by the solution-gate FET biosensor, and hybrid nanostructures, combined by the CVD-Graphene and MoS_2 layers, were used as the sensing material, which is illustrated in Fig. 2a. MoS_2 layers, which were used as a protective layer to avoid the noise caused by water, allow the PBASE linker to be fixed though π-π coordination interaction between the MoS_2 surface and the pyrene group (Huang et al., 2016; Mei et al., 2018). The succinimide portion of PBASE protrudes from the surface of MoS_2 and allows the 5′-amine-modified Probe DNA to be fixed by the conjugation reaction between the amine group of Probe DNA and the amine-reactive succinimide group of PBASE, as shown in Fig. 2b. Compared with Fig. S6a, SEM image in the inset of Fig. 2c and the EDS images in Fig. S1 show that multilayer MoS_2 nanostructures were successfully formed on the graphene surface. The Raman spectrum (Fig. 2c) of graphene displayed a weak D peak and the intensity of 2D peak/the intensity of G peak is 1.556, indicating that graphene is single layer with few defects and has high carrier mobility (Shang et al., 2008; Yang et al., 2016). There are also two representative peaks at ~379 cm^{-1} and ~404 cm^{-1} (Li et al., 2016), which indicate MoS_2 successfully covered the graphene surface through van der Waals interactions (Yang et al., 2015; Zhou et al., 2014). The electrical characteristics of the MoS_2/graphene hybrid nanostructure FET device were obtained as shown in Fig. S2. They show the drain current increases with a slight reduction of the gate voltage, indicating that the device response is sensitive to the gate voltage and an ohmic contact between the graphene and ITO electrodes (Cai et al., 2014). DNA hybridization detection was measured by monitoring the voltage shift of the charge neutral point (ΔVCNP) and the change of drain current (ΔIds) of the MoS_2/-graphene FET sensor (Lin et al., 2013; Xu et al., 2019), which are shown in Fig. 2d.

3.2. Sensitivity

The sensitivity of the MoS_2/graphene FET biosensor was analyzed as shown in Fig. 3a and b. The limit of detection went down to 10 aM and a good linear relationship ($R^2 = 0.991$) was obtained, which demonstrates that such a sensor can effectively perform DNA detection. As seen from Fig. 3a, the I_{ds} of the device decreased as the concentration of complementary DNA increased from 1 aM to 100 pM. From the linear relationship represented by $\Delta Ids(\mu A) = -2.95\ lgC_{DNA}\ (aM) - 4.63$ ($R^2 = 0.991$), a DNA detection signal with a gradient concentration was obtained, which clearly reveals that the electrical conductivity decreased regularly as the DNA concentration increased from 1 aM to 100 pM. The detection signal of the lowest concentration of complementary DNA must be higher than the noise signal to be considered valid (Mei et al., 2018). The dashed line in Fig. 3b represents the noise level (13.2 μA) from the blank control test, but the signal level (11.4 μA) of DNA with 1 aM is lower than noise level, so the data at 1 aM DNA was not valid. LOD as low as 10 aM was determined basing this signal (15.0 μA) exceeded the noise level. The above results show that the LOD of the MoS_2/-graphene nanostructure FET sensor should be 10 aM.

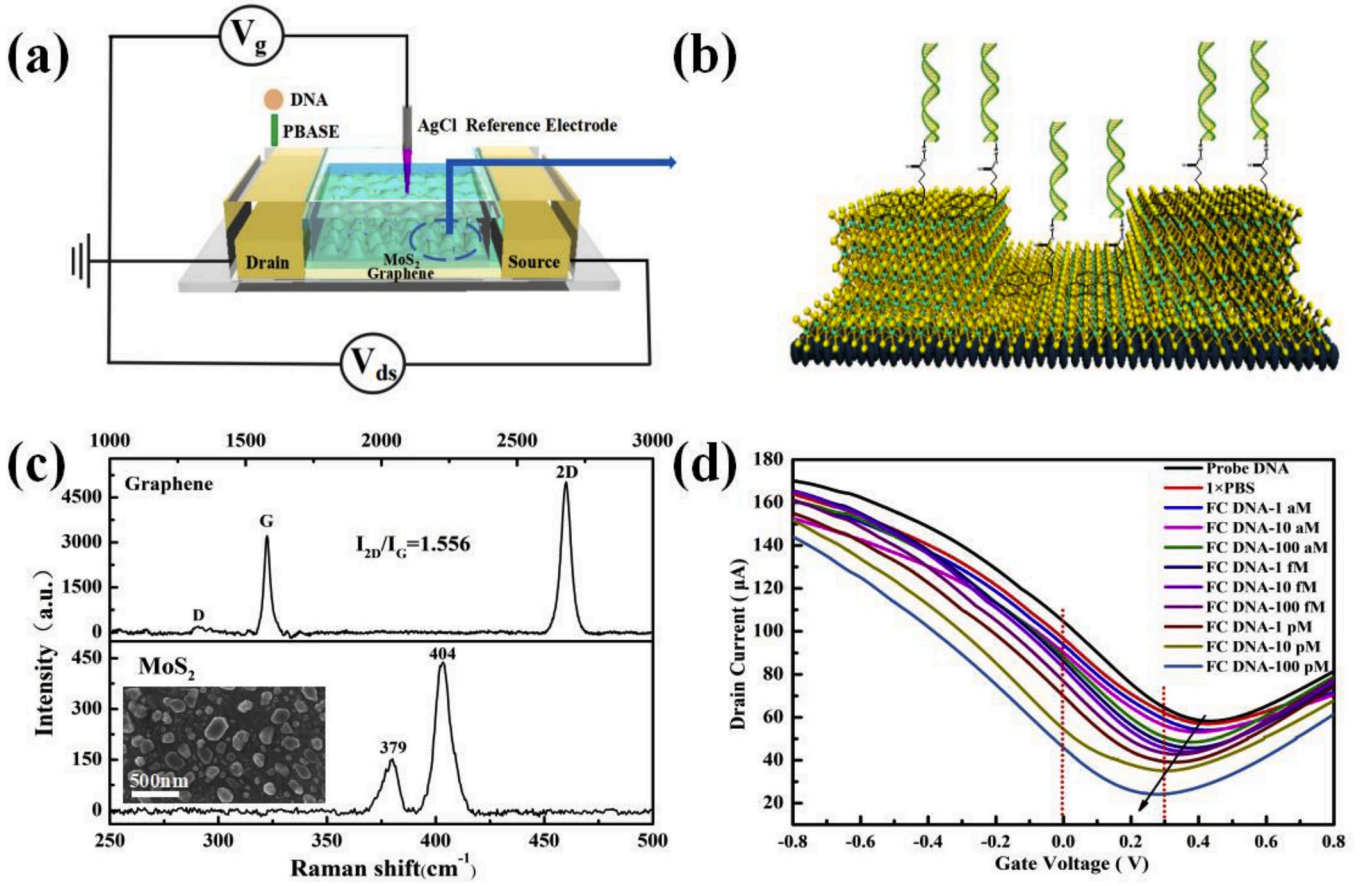

Fig. 2. (a) Schematic illustration of the MoS_2/graphene FET biosensor. (b) Schematic of the MoS_2/graphene nanostructure. (c) Raman spectrum of MoS_2/graphene, inset: SEM image of MoS_2 coated on the graphene surface. (d) Transfer characteristics curves for full-complementary DNA, for the different concentrations studied.

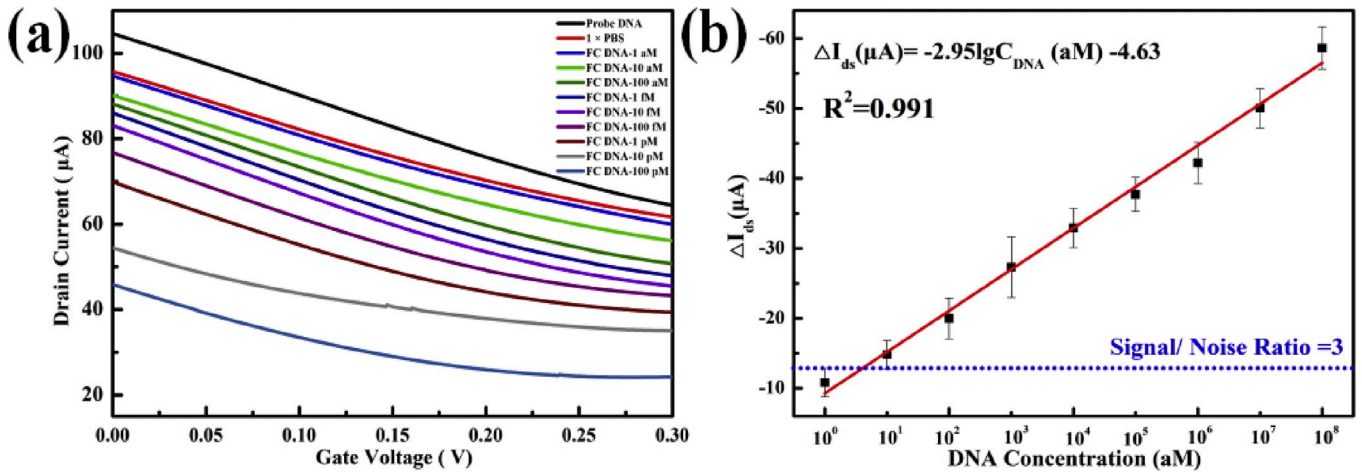

Fig. 3. (a) Linear regime of the transfer characteristics curves (V_g = 0–0.3 V). (b) A plot of I_{ds} decrease (ΔIds) versus logarithm of DNA concentration (C_{DNA}) in the range of 1 aM–100 pM with good linearity, R^2 = 0.991. Dashed line represents the triple noise level (13.2 μA) from the blank control test.

3.3. MoS_2/graphene nanostructure sensing mechanism

ΔVCNP was studied as another detection signal to further discuss the LOD. From a linear relationship represented by ΔVCNP(mV) = −18.3 lgC_{DNA} (aM) −3.0 (R^2 = 0.996), the DNA detection signal with the gradient concentration was obtained as shown in Fig. 4a, which clearly reveals that ΔVCNP increased regularly as DNA concentration increased from 1 aM to 100 pM. The detection signal level (4.5 mV) of the 1 aM DNA was lower than the noise signal level (9.8 mV), which was less than 10 aM DNA (20.7 mV). LOD of 10 aM was confirmed again from the ΔVCNP data.

Two mechanisms, the negative electrostatic gating effect and donor effect, can effect ΔVCNP(Guo et al., 2011; Kim et al., 2019). The negative electrostatic gating effect, where negatively charged DNA molecules can introduce positive charges on the sensing materials (Dong et al., 2010; Kim et al., 2019; Li et al., 2011), is shown in Fig. 4b_1. Note that the

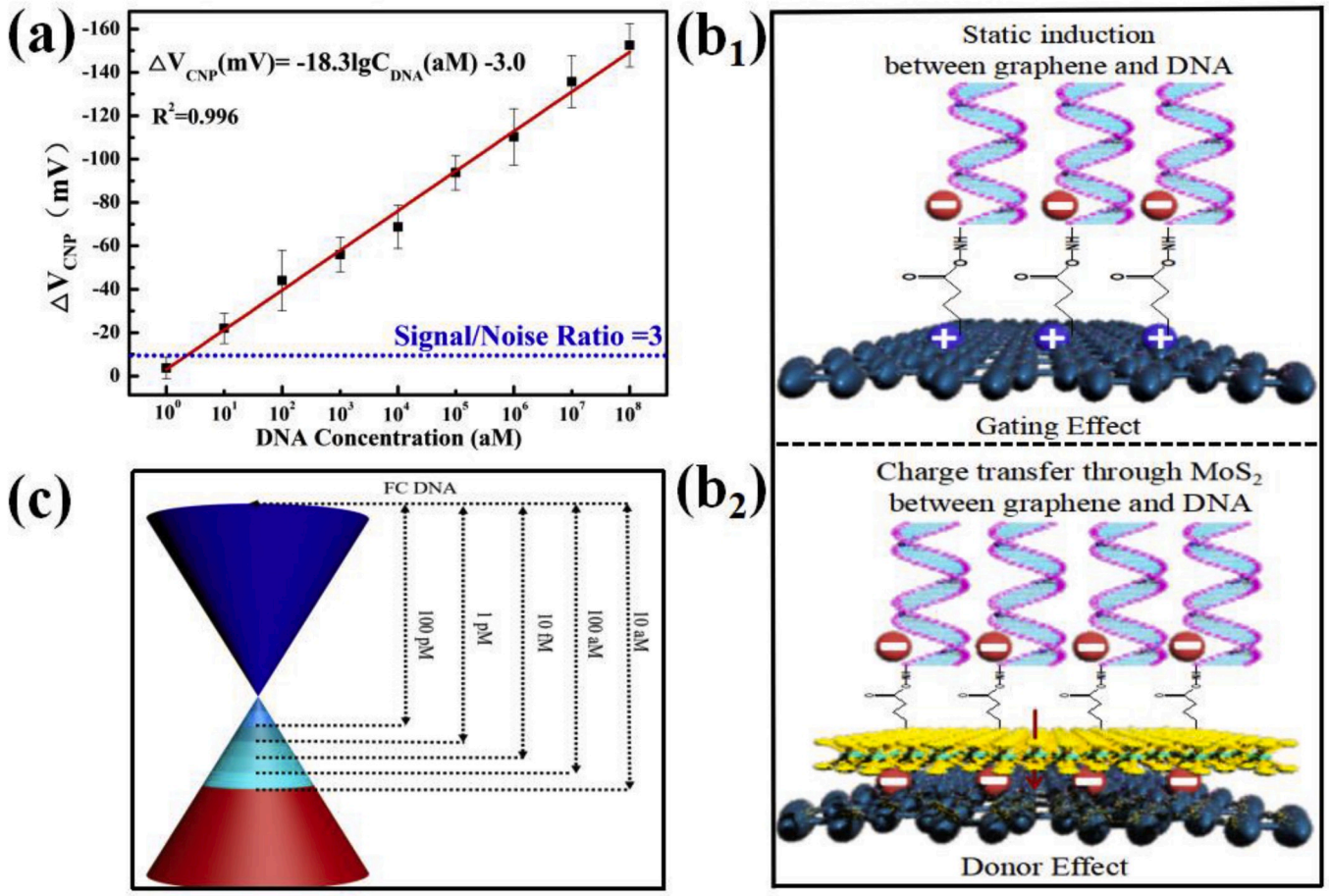

Fig. 4. (a) ΔVCNP was plotted as a function of DNA concentration. Dashed line represents the triple noise level (9.8 mV) from the blank control test. (b) Schematic of the gating effect (b_1) and donor effect (b_2). (c) Schematic illustration of the Fermi level after DNA hybridization.

obtained graphene is p type (shown in Fig. S2a), and such an effect increases the carrier density of the sensing material and makes the Fermi level move away from the Dirac point, and the charge neutral point moves in the positive direction (Campos et al., 2019), as shown in Fig. S3a. The donor effect represents the sensing material directly accepting electrons from DNA (Fig. 4b$_2$). Such an effect causes the sensing material to be N doped. The tapering carrier density of graphene causes the Fermi level to move closer to the Dirac point and the charge neutral point to move in the negative direction (Cai et al., 2014; Dong et al., 2010; Hwang et al., 2018), as shown in Fig. S3b.

The donor effect is the main mechanism for our proposed MoS_2/graphene nanostructure FET sensor. MoS_2 layers, with special charge distribution, can easily induce polarization of the DNA molecules (Wu et al., 2013). The mutual attraction of the polarized MoS_2 and DNA reduces the distance between them. Electrons of the negatively charged DNA groups are easily transferred to the MoS_2/graphene nanostructure. The charge neutral point moves to the negative direction, as shown in Figs. 2d and 4a.

More importantly, the ΔVCNP of our proposed FET is bigger than that of the graphene FET sensor (Fig. S4), benefiting from that the donor effect in the MoS_2/graphene nanostructure overcomes the shortcoming (Debye shielding) caused by gating effect (Dankerl et al., 2010; Gao et al., 2015, 2016). In a graphene based solution-gate FET sensor, the changes of carrier density that are mainly modulated by the DNA's gating effect are recognized as detection signal (Guo et al., 2011; Yue et al., 2017). However, limited by the Debye shielding effect, only part of the DNA within the Debye length can modulate the carrier density, so the DNA detection signal is weak (Campos et al., 2019; Nakatsuka et al., 2018).

In the proposed MoS_2/graphene based solution-gate FET sensor, MoS_2 (polar molecule) can easily induce the polarization of DNA molecules (nonpolar molecule), produce induced dipole moments, and reduce the distance between DNA and the sensing materials. MoS_2, which is relatively abundant in electrons, can easily form π−π interactions with DNA, which is relatively lacking in electrons (Huang et al., 2016; Li et al., 2015; Lu et al., 2017; Min et al., 2011; Yang et al., 2015), and permits the modulation of DNA to the sensing material to be performed by direct charge transfer, which is not affected by the gating effect. More MoS_2 molecules will polarize more DNA molecules, which leads to more and more DNA molecules regulating the carrier density of the sensing material by the donor effect, which gradually replaces the gating effect as the $(NH_4)_2MoS_4$ solution concentration increases.

3.4. Modulation of doping degree of MoS_2 for sensing mechanism

Whether the gating or donor effect plays a leading role in the MoS_2/graphene FET sensor depends on the doping degree of the MoS_2 to graphene, which can be altered by using different concentrations of $(NH_4)_2MoS_4$ solution. We believed that the gating effect of DNA to the sensing material remained constant due to the fact that there is no change in the electrolyte, while the donor effect can be modulated by the introduction of MoS_2. When the doping degree was weak (low concentration of $(NH_4)_2MoS_4$ solution), the gating effect was bigger than the donor effect. The charge neutral point moves in the positive direction and a small ΔVCNP occurred, as shown in section A of Fig. 5a and mark 1 of Fig. 5b. When the concentration of $(NH_4)_2MoS_4$ solution increased from 0.01 g/ml to 0.06 g/ml, the donor effect played a larger role than the gating effect in modulating the carrier density because more MoS_2 was synthesized, further enhancing the donor effect. In this case, the charge neutral point gradually moves in the negative direction and a larger ΔVCNP occurred, as shown in section B of Fig. 5a and mark 2 of Fig. 5b. When the concentration of the $(NH_4)_2MoS_4$ solution reached a certain value (0.1 g/ml), a MoS_2 negatively charged block was formed, which worked as a scattering center that weakened carrier mobility and decreased ΔVCNP (Wang et al., 2015), as shown in section C of Fig. 5a.

3.5. Specificity

The selective specificity of the MoS_2/graphene FET biosensor is analyzed as shown in Fig. 6a and b. Complementary DNA with five matching degrees was accurately recognized, which proves that the sensor can effectively perform DNA detection. As seen from Fig. 6a, a different shift of the charge neutral point occurred after adding five matching degrees of complementary DNA. The quantified amount of ΔVCNP is shown in Fig. 6b. ΔVCNP increased as the matching degrees of complementary DNA increased, due to more complementary DNA being specifically adsorbed by hybridization with the Probe DNA. When 15Ms DNA was used to hybridize with the Probe DNA, a small ΔVCNP occurred, which can be attributed to nonspecific adsorption between the 15Ms DNA and the Probe DNA (Allen et al., 2007; Yin et al., 2012), The signal of the Probe DNA + 1Ms DNA was dramatically weaker than that of the Probe DNA + FC DNA because they formed a double helix structure after hybridization that was unstable and easily damaged during the washing steps (Mei et al., 2018). The obtained results are in good agreement with the previously reported results (Kaisti et al., 2017; Sorgenfrei et al., 2011), which confirms that the MoS_2/graphene FET can detect DNA specificity.

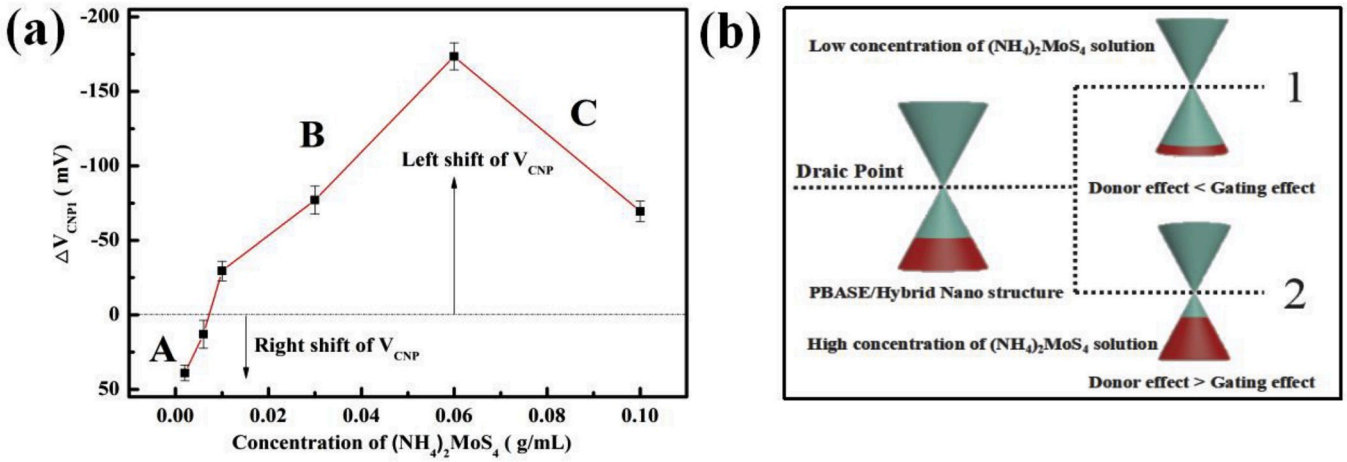

Fig. 5. (a) ΔVCNP shifting of the samples with different doping effect. The samples was grown at 500 °C with a growth concentration of 0.001 g/ml, 0.003 g/ml, 0.006 g/ml, 0.01 g/ml, 0.03 g/ml, 0.06 g/ml, 0.08 g/ml, 0.1 g/ml. ΔVCNP1(mV) = $V_{CNP\ (Probe\ DNA)}$ -$V_{CNP\ (Hybrid\ Nanostructure)}$. (b) Schematic diagram of the graphene Fermi level modulation mechanism in MoS_2/graphene nanostructure FET.

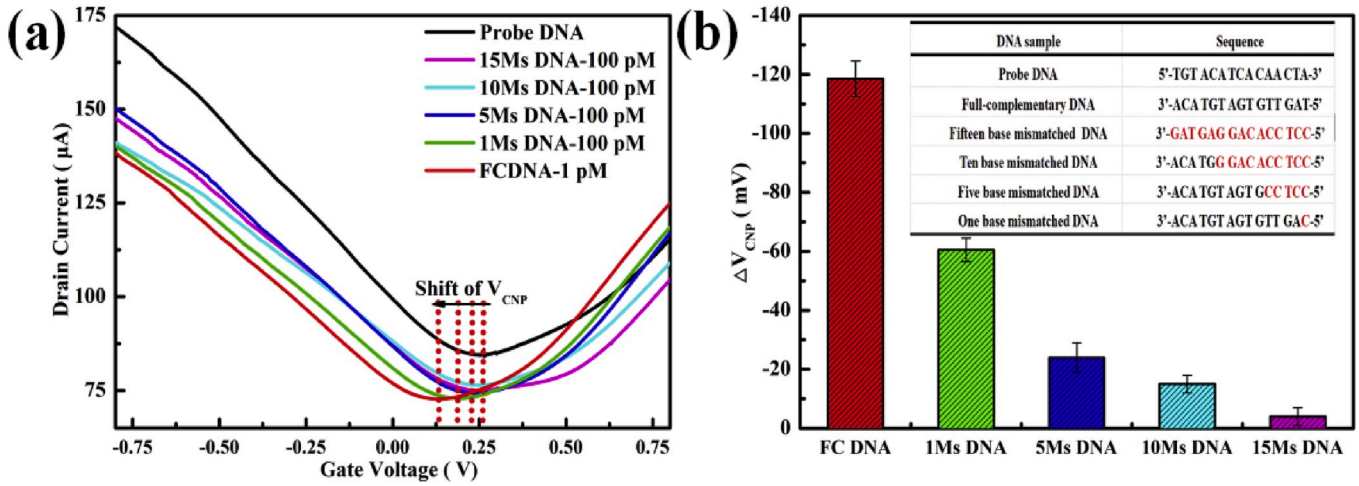

Fig. 6. (a) Transfer characteristics of the MoS_2/graphene FET biosensor incubated with 1 pM FCDNA and 100 pM one-base mismatched DNA (1MsDNA), five-bases mismatched DNA (5MsDNA), 10-bases mismatched DNA (10MsDNA), and 15-bases mismatched DNA (15MsDNA). (b) The ΔVCNP shift of the samples with different matching degrees of complementary DNA, inset: DNA sample sequence.

4. Conclusions

In this study, a MoS_2/graphene FET sensor, where MoS_2 works as a barrier layer from the electrolyte to graphene and closes the distance between DNA and the sensing material by polarizing the DNA molecules, was introduced to weaken the noise signal and enhance the DNA detection signal. A competitive sensing mechanism of the proposed sensor was established and discussed where the donor effect played a leading role in the DNA sensing signal. High sensitivity (LOD of 10 aM) and selective specificity (complementary DNA with five matching degrees was accurately recognized) were obtained by the sensor. The developed FET sensor can be integrated with other devices to realize a lab-on-a-chip due to its various advantages such as stable signal, low cost, and small dimension. If such a biosensor can be functionalized by a multi-channel and microfluidic system in the future, it's potential in disease diagnosis and treatment would be further enhanced.

Declaration of competing interest

The authors declare that they have no known competing financial interests or personal relationships that could have appeared to influence the work reported in this paper.

CRediT authorship contribution statement

Shuo Chen: Conceptualization, Methodology, Software, Validation, Formal analysis, Investigation, Resources, Data curation, Writing - original draft, Visualization. **Yang Sun:** Conceptualization, Methodology, Software, Validation, Formal analysis, Investigation, Resources, Data curation, Writing - original draft, Visualization. **Yaping Xia:** Methodology, Investigation. **Ke Lv:** Formal analysis, Software. **Baoyuan Man:** Conceptualization, Writing - review & editing, Supervision. **Cheng Yang:** Conceptualization, Formal analysis, Resources, Data curation, Writing - review & editing, Supervision, Project administration, Funding acquisition.

Acknowledgments

The authors are grateful for financial support from the National Natural Science Foundation of China (11874244, 11974222), Key Research and Development Plan of Shandong Province (No. 2019GGX102048).

Appendix A. Supplementary data

Supplementary data to this article can be found online at https://doi.org/10.1016/j.bios.2020.112128.

References

Allen, B.L., Kichambare, P.D., Star, A., 2007. Carbon nanotube field-effect-transistor-based biosensors. Adv. Mater. 19 (11), 1439–1451.
Cai, B., Wang, S., Huang, L., Ning, Y., Zhang, Z., Zhang, G.-J., 2014. Ultrasensitive label-free detection of PNA–DNA hybridization by reduced graphene oxide field-effect transistor biosensor. ACS Nano 8 (3), 2632–2638.
Campos, R., Borme, J., Guerreiro, J.R., Machado Jr., G., Cerqueira, M.F.t., Petrovykh, D. Y., Alpuim, P., 2019. Attomolar label-free detection of DNA hybridization with electrolyte-gated graphene field-effect transistors. ACS Sens. 4 (2), 286–293.
Dankerl, M., Hauf, M.V., Lippert, A., Hess, L.H., Birner, S., Sharp, I.D., Mahmood, A., Mallet, P., Veuillen, J.Y., Stutzmann, M., 2010. Graphene solution-gated field-effect transistor array for sensing applications. Adv. Funct. Mater. 20(18), 3117–3124.
Dong, X., Shi, Y., Huang, W., Chen, P., Li, L.J., 2010. Electrical detection of DNA hybridization with single-base specificity using transistors based on CVD-grown graphene sheets. Adv. Mater. 22 (14), 1649–1653.
Du, X., Skachko, I., Barker, A., Andrei, E.Y., 2008. Approaching ballistic transport in suspended graphene. Nat. Nanotechnol. 3 (8), 491.
Fradetal, L., Bano, E., Attolini, G., Rossi, F., Stambouli, V., 2016. A silicon carbide nanowire field effect transistor for DNA detection. Nanotechnology 27 (23), 235501.
Gao, N., Gao, T., Yang, X., Dai, X., Zhou, W., Zhang, A., Lieber, C.M., 2016. Specific detection of biomolecules in physiological solutions using graphene transistor biosensors. Proc. Natl. Acad. Sci. U. S. A. 113(51), 14633–14638.
Gao, Z., Xia, H., Zauberman, J., Tomaiuolo, M., Ping, J., Zhang, Q., Ducos, P., Ye, H., Wang, S., Yang, X., 2018. Detection of sub-fM DNA with target recycling and self-assembly amplification on graphene field-effect biosensors. Nano Lett. 18 (6), 3509–3515.
Gao, N., Zhou, W., Jiang, X., Hong, G., Fu, T.-M., Lieber, C.M., 2015. General strategy for biodetection in high ionic strength solutions using transistor-based nanoelectronic sensors. Nano Lett. 15(3), 2143–2148.
Guo, S.-R., Lin, J., Penchev, M., Yengel, E., Ghazinejad, M., Ozkan, C.S., Ozkan, M., 2011. Label free DNA detection using large area graphene based field effect transistor biosensors. J. Nanosci. Nanotechnol. 11 (6), 5258–5263.
Huang, Y., Zheng, W., Qiu, Y., Hu, P., 2016. Effects of organic molecules with different structures and absorption bandwidth on modulating photoresponse of MoS_2 photodetector. ACS Appl. Mater. Interfaces 8 (35), 23362–23370.
Hwang, M.T., Wang, Z., Ping, J., Ban, D.K., Shiah, Z.C., Antonschmidt, L., Lee, J., Liu, Y., Karkisaval, A.G., Johnson, A.T.C., 2018. DNA nanotweezers and graphene transistor enable label-free genotyping. Adv. Mater. 30 (34), 1802440.
Jayakumar, G., Legallais, M., Hellstrom, P.-E., Mouis, M., Pignot-Paintrand, I., Stambouli-Sene, V., Ternon, C., Östling, M., 2019. Wafer-scale HfO_2 Encapsulated Silicon Nanowire Field Effect Transistor for Efficient Label-free DNA Hybridization Detection in Dry Environment. Nanotechnology.
Kaisti, M., 2017. Detection principles of biological and chemical FET sensors. Biosens. Bioelectron. 98, 437–448.
Kelley, S.O., Mirkin, C.A., Walt, D.R., Ismagilov, R.F., Toner, M., Sargent, E.H., 2014. Advancing the speed, sensitivity and accuracy of biomolecular detection using multi-length-scale engineering. Nat. Nanotechnol. 9 (12), 969.

Khosravi, F., Loeian, S., Panchapakesan, B., 2017. Ultrasensitive label-free sensing of IL-6 based on PASE functionalized carbon nanotube micro-arrays with RNA-aptamers as molecular recognition elements. Biosens. Bioelectron. 7 (2), 17.
Kim, D.-J., Sohn, I.Y., Jung, J.-H., Yoon, O.J., Lee, N.-E., Park, J.-S., 2013. Reduced graphene oxide field-effect transistor for label-free femtomolar protein detection. Biosens. Bioelectron. 41, 621–626.
Kim, H.E., Schuck, A., Lee, J.H., Kim, Y.-S., 2019. Solution-gated graphene field effect transistor for TP53 DNA sensor with coplanar electrode array. Sensor. Actuator. B Chem. 291, 96–101.
Li, Y., Chen, S., Kaneko, T., Hatakeyama, R., 2011. Electrically moving single-stranded DNA into and out of double-walled carbon nanotubes. Chem. Commun. 47 (8), 2309–2311.
Li, Z., Jiang, S., Xu, S., Zhang, C., Qiu, H., Li, C., Sheng, Y., Huo, Y., Yang, C., Man, B., 2016. Few-layer MoS_2-encapsulated Cu nanoparticle hybrids fabricated by two-step annealing process for surface enhanced Raman scattering. Sensor. Actuator. B Chem. 230, 645–652.
Li, Z., Ye, R., Feng, R., Kang, Y., Zhu, X., Tour, J.M., Fang, Z., 2015. Graphene quantum dots doping of MoS_2 monolayers. Adv. Mater. 27 (35), 5235–5240.
Lin, C.T., Loan, P.T.K., Chen, T.Y., Liu, K.K., Chen, C.H., Wei, K.H., Li, L.J., 2013. Label-Free Electrical detection of DNA hybridization on graphene using Hall Effect measurements: revisiting the sensing mechanism. Adv. Funct. Mater. 23 (18), 2301–2307.
Loan, P.T.K., Zhang, W., Lin, C.T., Wei, K.H., Li, L.J., Chen, C.H., 2014. Graphene/MoS_2 heterostructures for ultrasensitive detection of DNA hybridisation. Adv. Mater. 26 (28), 4838–4844.
Long, C., McAnally, J.R., Shelton, J.M., Mireault, A.A., Bassel-Duby, R., Olson, E.N., 2014. Prevention of muscular dystrophy in mice by CRISPR/Cas9–mediated editing of germline DNA. Science 345 (6201), 1184–1188.
Lu, C., Liu, Y., Ying, Y., Liu, J., 2017. Comparison of MoS_2, WS_2, and graphene oxide for DNA adsorption and sensing. Langmuir 33 (2), 630–637.
Mei, J., Li, Y.-T., Zhang, H., Xiao, M.-M., Ning, Y., Zhang, Z.-Y., Zhang, G.-J., 2018. Molybdenum disulfide field-effect transistor biosensor for ultrasensitive detection of DNA by employing morpholino as probe. Biosens. Bioelectron. 110, 71–77.
Min, S.K., Kim, W.Y., Cho, Y., Kim, K.S., 2011. Fast DNA sequencing with a graphene-based nanochannel device. Nat. Nanotechnol. 6 (3), 162.
Nakatsuka, N., Yang, K.-A., Abendroth, J.M., Cheung, K.M., Xu, X., Yang, H., Zhao, C., Zhu, B., Rim, Y.S., Yang, Y., 2018. Aptamer–field-effect transistors overcome Debye length limitations for small-molecule sensing. Science 362 (6412), 319–324.
Schedin, F., Geim, A., Morozov, S., Hill, E., Blake, P., Katsnelson, M., Novoselov, K., 2007. Detection of individual gas molecules adsorbed on graphene. Nat. Mater. 6 (9), 652.
Shang, N.G., Papakonstantinou, P., McMullan, M., Chu, M., Stamboulis, A., Potenza, A., Dhesi, S.S., Marchetto, H., 2008. Catalyst-free efficient growth, orientation and biosensing properties of multilayer graphene nanoflake films with sharp edge planes. Adv. Funct. Mater. 18 (21), 3506–3514.
Sorgenfrei, S., Chiu, C.-y., Gonzalez Jr., R.L., Yu, Y.-J., Kim, P., Nuckolls, C., Shepard, K. L., 2011. Label-free single-molecule detection of DNA-hybridization kinetics with a carbon nanotube field-effect transistor. Nanotechnology 6 (2), 126.
Stern, E., Wagner, R., Sigworth, F.J., Breaker, R., Fahmy, T.M., Reed, M.A., 2007. Importance of the Debye screening length on nanowire field effect transistor sensors. Nano Lett. 7 (11), 3405–3409.
Sun, Y., Peng, Z., Li, H., Wang, Z., Mu, Y., Zhang, G., Chen, S., Liu, S., Wang, G., Liu, C., 2019. Suspended CNT-Based FET sensor for ultrasensitive and label-free detection of DNA hybridization. Biosens. Bioelectron. 137, 255–262.
Wang, J., Li, S., Zou, X., Ho, J., Liao, L., Xiao, X., Jiang, C., Hu, W., Wang, J., Li, J., 2015. Integration of high-k oxide on MoS_2 by using ozone pretreatment for high-performance MoS_2 top-gated transistor with thickness-dependent carrier scattering investigation. Small 11 (44), 5932–5938.
Wu, S., Huang, C., Aivazian, G., Ross, J.S., Cobden, D.H., Xu, X., 2013. Vapor–solid growth of high optical quality MoS_2 monolayers with near-unity valley polarization. ACS Nano 7 (3), 2768–2772.
Xu, S., Zhan, J., Man, B., Jiang, S., Yue, W., Gao, S., Guo, C., Liu, H., Li, Z., Wang, J., 2017. Real-time reliable determination of binding kinetics of DNA hybridization using a multi-channel graphene biosensor. Nat. Commun. 8, 14902.
Xu, S., Zhang, C., Jiang, S., Hu, G., Li, X., Zou, Y., Liu, H., Li, J., Li, Z., Wang, X., 2019. Graphene foam field-effect transistor for ultra-sensitive label-free detection of ATP. Sensor. Actuator. B Chem. 284, 125–133.
Yang, C., Zhang, C., Huo, Y., Jiang, S., Qiu, H., Xu, Y., Li, X., Man, B., 2016. Shell-isolated graphene@ Cu nanoparticles on graphene@ Cu substrates for the application in SERS. Carbon 98, 526–533.
Yang, M., Jeong, J.-M., Huh, Y.S., Choi, B.G., 2015. High-performance supercapacitor based on three-dimensional MoS_2/graphene aerogel composites. Compos. Sci. Technol. 121, 123–128.
Yin, Z., He, Q., Huang, X., Zhang, J., Wu, S., Chen, P., Lu, G., Zhang, Q., Yan, Q., Zhang, H., 2012. Real-time DNA detection using Pt nanoparticle-decorated reduced graphene oxide field-effect transistors. Nanoscale 4 (1), 293–297.
Yue, W., Tang, C., Wang, C., Bai, C., Liu, S., Xie, X., Hua, H., Zhang, Z., Li, D., 2017. An electricity-fluorescence double-checking biosensor based on graphene for detection of binding kinetics of DNA hybridization. RSC Adv. 7 (70), 44559–44567.
Zhou, W., Zhou, K., Hou, D., Liu, X., Li, G., Sang, Y., Liu, H., Li, L., Chen, S., 2014. Three-dimensional hierarchical frameworks based on MoS_2 nanosheets self-assembled on graphene oxide for efficient electrocatalytic hydrogen evolution. ACS Appl. Mater. Interfaces 6 (23), 21534–21540.